ELSEVIER

Contents lists available at ScienceDirect

Nuclear Inst. and Methods in Physics Research, B

journal homepage: www.elsevier.com/locate/nimb





Combining PIXE and EBS for the analysis of paint layers: Experiment and simulation highlight the influence of the pigment grain size

Lucile Beck ^{a,*}, Matej Mayer ^b, Tiago F. Silva ^c, Claire Berthier ^d, Laurent Pichon ^{e,f}

- ^a LMC14, LSCE/IPSL, CEA-CNRS-UVSQ, Université Paris-Saclay, 91191 Gif-sur-Yvette, France
- ^b Max-Planck-Institut für Plasmaphysik, 85748 Garching, Germany
- ^c Instituto de Fisica da Universidade de Sao Paulo, 05508-090 Sao Paulo, Brazil
- ^d INSTN, CEA Saclay, Université Paris-Saclay, 91191 Gif-sur-Yvette, France
- ^e Centre de Recherche et de Restauration des Musées de France, Palais du Louvre, 75001 Paris, France
- f Fédération de Recherche NewAGLAE, FR3506 CNRS/MC/UPMC, Palais du Louvre, 75001 Paris, France

ARTICLE INFO

Keywords:

PIXE

RBS

EBS

Painting

Pigment

Grain size

ABSTRACT

PIXE and EBS were used simultaneously to characterize paint layers containing pigments of controlled grain size. The experiments were carried out using the external 3 MeV proton beam from the NewAGLAE facility. The paint layers consisted of lead silicate pigments mixed in linseed oil. The pigments were characterized by XRD and SEM prior to IBA measurements. Irregularly shaped grains ranging from 13 to 64 µm were observed.

The PIXE spectra were fitted by TRAUPIXE and the EBS spectra were simulated with STRUCTNRA using simplified models of the paint structure assuming non-overlapping spherical pigment particles in oil. For each simulation, the particle size was used as provided by the SEM observations. The density of each paint layer was calculated according to the pigment composition determined by PIXE. For the linseed oil matrix, the oxygen content was fitted at about two times higher than in linseed oil, which is qualitatively consistent with the oxygen uptake during the drying process. The pigment volume fraction and the stick-out fraction were adjusted to fit the experimental spectra. A reasonable agreement between experimental and simulated spectra was achieved. This demonstrates that the simulation and quantitative understanding of EBS spectra from paintings requires the microstructure of the paint layer to be taken into account.

1. Introduction

Up to now, Ion Beam Analysis (IBA) has been used only occasionally for analyzing paintings [1–7] for two main reasons: quantitative analysis is sometimes difficult to interpret due to the complex structure of the paint layers and, in some cases, a visible modification of the surface has been observed under ion beam irradiation [8–12].

To improve the characterization of paintings, it was proposed some years ago to combine elastic backscattering spectrometry (EBS) and particle-induced X-ray emission (PIXE) simultaneously [13,14], in order to collect complementary data such as pigment composition and layer thickness and quantify the organic binder proportion [15]. Simultaneous PIXE and EBS experiments also have the advantages of limiting the beam exposure and providing information on both pigment(s) and binder in one experiment. This combination, implemented with the AGLAE external beam, was successfully applied to paintings and to

painting cross-sections for the study of Italian Renaissance masterpieces [16]

However, fitting EBS spectra is not straightforward when it comes to analyzing paintings. Attempts to use artificial devices that introduce extra energy loss through an invisible element (H) [17] or a roughness algorithm [18] have been explored. Furthermore, Mayer and Silva [19] using computer simulations pointed out that the shape of EBS spectra also depends on the microstructure of the paint layer. They calculated EBS spectra of idealized paint layers of lead white (PbCO₃) in linseed oil using the STRUCTNRA code [20], producing different spectra as a function of pigment particle diameter and concentration. They concluded that an accurate quantitative evaluation of backscattering spectra from paint requires taking the correct microstructure of the paint layer into account. It was also demonstrated that the homogeneity assumption leads to errors in the quantification of the elements, as the derived concentrations depend on the shape and size of the

E-mail address: lucile.beck@cea.fr (L. Beck).

 $^{^{\}ast}$ Corresponding author.

microstructure. These conclusions are important since they may limit the application and validity of IBA results on artworks given the current status of standard tools of data processing. To increase confidence in IBA and its applicability in this field, more studies are necessary.

The aim of this paper was to reproduce the simulations experimentally. For that purpose, various replications of paint containing pigments of controlled grain sizes were mixed in linseed oil and characterized using XRD and SEM prior to IBA measurements. PIXE and EBS were carried out using a 3 MeV proton beam and BS spectra were fitted with the STRUCTNRA code using simplified models of the paint structure assuming non-overlapping spherical pigment particles in oil.

2. Material and methods

2.1. Controlled paint layers: preparation and characterization

To reproduce the previous simulations described in Mayer and Silva [19], lead white or lead carbonates (PbCO $_3$ and 2PbCO $_3$.Pb(OH) $_2$) with controlled particle size were sought. However, due to lack of availability, lead silicates produced by the Nakagawa Gofun Enogu company were chosen as the closest match.

The manufacturing process developed by this company ensures a controlled grain size for each pigment [21,22]. During production, pigment powders are sorted by grade depending on particle size and classified according to standardization numbers. The smaller the number, the larger the particle and the darker the color; the higher the number, the smaller the particle and the lighter the color. According to the supplier, number 8 corresponds approximately to an average grain size of 50 μm , number 10 to 27 μm and number 12 to 14 μm .

Three pigments named *Iwaaka*, *Iwaki* and *Gunjo* (red, yellow and blue), each with three different grain sizes (8, 10, 12), were characterized by optical microscopy, scanning electron microscopy (SEM) and X-ray diffraction (Beck et al. in preparation). SEM was used to determine the main elements, to observe the grain morphology and to measure the mean grain size.

Thick paint layers were prepared by mixing each pigment (red, yellow or blue) with linseed oil in controlled proportions. For each pigment, three grain sizes (8, 10, 12) were used. In total, nine samples of thick paint layers were prepared.

2.2. PIXE and EBS experiments

PIXE and EBS were carried out simultaneously using the external 3 MeV proton beam of the NewAGLAE accelerator at the Centre de Recherche et de Restauration des Musées de France (Louvre Palace, Paris, France) [23]. The beamline nozzle ends with a 100 nm thick Si_3N_4 window, representing the interface with the atmosphere, and the samples were placed at a working distance of a few millimeters.

For the PIXE mode, four Peltier-cooled SDD-EDX detectors were used. One is dedicated to low energy X-rays (1–10 keV). It is equipped with a permanent magnet deflector to protect the crystal from back-scattered particles and a helium flow to improve low energy X-ray transmission. The other three detectors are dedicated to high energy X-rays (3–40 keV), usually employed to measure trace elements. They are protected from backscattered particles with interchangeable filters. Aluminum filters were used for this experiment. EBS measurements were performed with a detector collecting backscattered protons at 130° with respect to the incident beam.

PIXE spectra were fitted by TRAUPIXE [24]. The TRAUPIXE program uses the GUPIXWIN [25] calculation engine (executable PIXWIN.EXE) to process each analyzed point sequentially with matrix and trace solutions. It dynamically manages the GUPIX engine through the GUPIX-WIN.PAR parameter file, retrieves results from the GUPIX output files and writes all the results in a single Excel file. This file contains elemental and oxide concentrations and limits of detection (LOD).

The EBS spectra were simulated with STRUCTNRA [19].

STRUCTNRA is a computer code for the simulation of scattering or recoil spectra from samples with structure, such as gratings or multicomponent materials. It uses the well-known and widely used SIMNRA code as simulation kernel [26] and has been benchmarked with experimental spectra and a variety of other codes [27].

2.3. Model and assumptions for the EBS simulation

The paint microstructure used in the STRUCTNRA model consisted of two phases, the pigment and the surrounding matrix, the organic binder. Pigment particles were assumed to be spherical, the diameter of the spheres was assumed to follow a Gaussian distribution with mean diameter and standard deviation provided by the SEM results. The pigment particles are non-overlapping and distributed randomly in 3D with periodic boundary conditions parallel to the surface. At the surface, the pigment particles can stick out from the surface up to some percentage of their diameter; this 'stick-out' fraction was used as a fit parameter. The 2-dimensional cross-section of each sample was used for the simulations with a pixel size of 1 x 1 μm^2 . An individual simulation typically takes around 10 min on a computer with 32 cores using 64 threads in parallel, which corresponds to a few hours on a single core computer.

For the pigment particles, the composition of medium and high-Z elements as determined by PIXE was used, while the amount of oxygen in the pigment was based on the knowledge of the composition of medium and high-Z elements and the assumptions described below. The base material was lead silicate glass with a composition of PbO · nSiO₂, where n was determined from the PIXE results for Pb and Si and was close to 1. The mass density was taken from Alderman et al., 2022 [28]. The red color was cadmium sulfide selenide, a mixture of CdS and CdSe. The CdS:CdSe ratio was taken from the PIXE results for Cd and Se and was found typically to be around 3, as densities 5.81 g/cm³ (CdSe) and 4.65 g/cm³ (CdS) were used. S could not be determined from the PIXE spectra due to overlap of the S_K line with the $\mbox{\rm Pb}_M$ line. The amount of Swas therefore derived from the amounts of Cd and Se assuming a mixture of CdS and CdSe. Additionally, minor amounts of Ti and K were observed, which were assumed to be due to TiO_2 (4.23 g/cm³) and K_2O (2.35 g/cm³). The matrix was composed of linseed oil, which is a mixture of linolenic acid $C_{18}H_{30}O_2$ (52-55 %), oleic acid $C_{18}H_{34}O_2$ (18–23 %), and linoleic acid $C_{18}H_{32}O_2$ (14–17 %). A mean composition of C₁₈H₃₁O₂ with a mass density of 0.93 g/cm³ was assumed. The nominal pigment volume concentration was based on the sample preparation (37 % for the Iwaaka/red paint) but this parameter can be adjusted during fitting due to a possible non-uniformity through the paint layer.

The beam was simulated according to the experimental conditions: 3 MeV $H^+,$ incident angle $\alpha=0^\circ,$ exit angle $\beta=50^\circ,$ scattering angle $\theta=130^\circ.$ SRIM-2003 stopping powers [29], SigmaCalc [30] non-Rutherford scattering cross-sections for elements from helium to silicon and Rutherford scattering cross-sections from sulfur to lead were used. This introduces some uncertainties for the simulation of scattering from S, K and Ti, because these cross-sections are probably non-Rutherford at 3 MeV. However, there are no reliable non-Rutherford cross-section data available for all isotopes at the angle and energy used here.

3. Results

3.1. Pigment characterization and grain size distribution

Three pigments named *Iwaaka*, *Iwaki* and *Gunjo* (red, yellow and blue) were examined. SEM and XRD results showed that they consist of lead silicate glass PbO·nSiO₂ combined with a colored component: CdSe + CdS for red (Fig. 1a), Sb for yellow, and Co for blue.

Examination of the grain surface revealed an angular morphology of glassy grains with broken edges (Fig. 1b). This observation is consistent with the manufacturing process, which involves the formation of a block

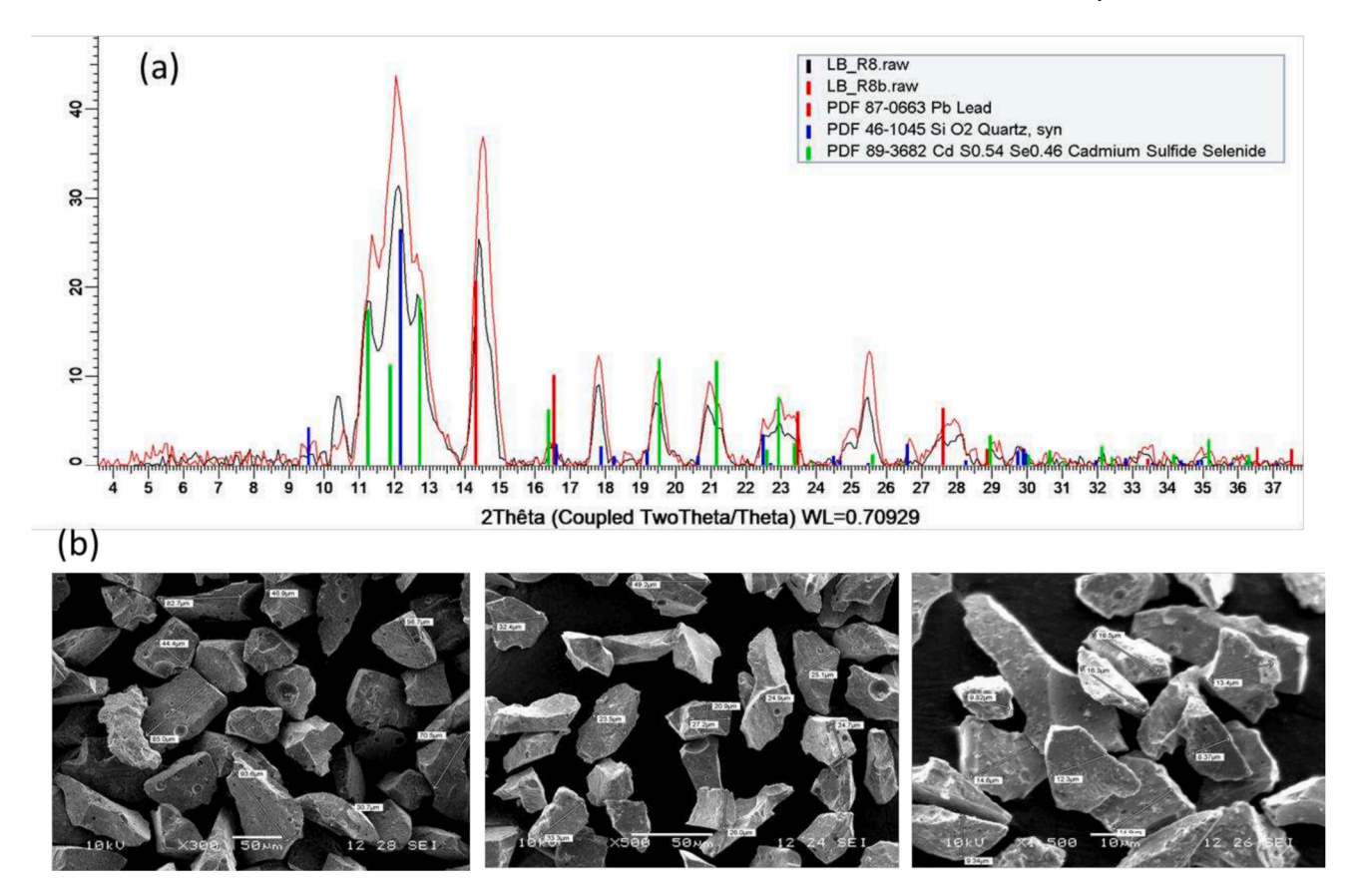


Fig. 1. (a) Two X-ray diffractograms (XRD) of the *Iwaaka*/red pigment, label 8 (red and black lines) compared to the reference materials lead, quartz and cadmium sulfide selenide (red, blue and green vertical bars, respectively); (b) From the left to the right, SEM images of the three *Iwaaka*/red pigments labelled 8, 10, 12 (the scale marks are 50 μm, 50 μm and 10 μm). Grain sizes are indicated in white rectangles.

of pigment by melting a colored component into a glaze matrix ($PbO \cdot nSiO_2$) and then its pulverization in a crusher to obtain different controlled grain sizes [21].

As the grain shape is irregular, the mean size values were calculated by taking into account the length and width of the grains. Mean grain sizes of $13\pm4\,\mu m$ (label 12), $26\pm4\,\mu m$ (label 10) and between 57 ± 8 and $64\pm20\,\mu m$ (label 8) were observed (Table 1). The two lowest values are in good agreement with the manufacturer's indication. For the coarser grain pigments, although the averages of the measured values are higher than the nominal value, they are statically compatible.

3.2. Paint layer analysis by PIXE

The composition (in wt%) of the nine samples of paint layer is summarized in Table 2. The PIXE results show that the lead silicate $\frac{1}{2}$

matrices have various molecular PbO/SiO $_2$ ratios from 0.5 to 2 consistent with the wide glass-forming range of the PbO-SiO $_2$ binary system [28]: PbO.2SiO $_2$ (yellow 12), 2PbO.3SiO $_2$ (red 12 and yellow 10), PbO. SiO $_2$ (red 8 and 10, yellow 8, 3PbO.2SiO $_2$ (blue 12) and 2PbO.SiO $_2$ (blue 8 and 10).

Contrary to expectations, pigments with the same name and visually identical color appear to have different compositions depending on grain size. These inconsistent results could be due to the differential absorption of the X-rays by the samples. SiO_2 concentrations tend to decrease with increasing grain size, which may indicate a stronger absorption of Si K X-rays (1.74 keV) with larger grain size. This effect, attributed to particle size and shape [31], is difficult to quantify in a multi-phase material such as paint and was not taken into account in the PIXE analysis.

The colored constituents observed by SEM or by XRD were confirmed

Table 1Grain size provided by the manufacturer and measured by SEM using the images of Fig. 1b.

Size label	8	10	12		
Estimated grain size provided by the manufacturer (µm)	∼50 µm	~27 µm	∼14 µm		
Measured mean and standard deviation (µm)	$64 \pm 23 \text{ (red)}$ $57 \pm 8 \text{ (yellow)}$ $68 \pm 20 \text{ (blue)}$	26 ± 4	13 ± 3		

Table 2
PIXE results for the nine samples of paint layer (in wt%). Concentrations for light elements and lead are given as oxide percentages. Elemental concentrations are reported for the other elements. Molecular PbO/SiO₂ ratios are calculated from weight concentrations.

	Grain size												PbO/SiO2
Pigment	label	PbO	SiO2	Na2O	Al2O3	K2O	Ti	Co	Zn	Se	Cd	Sb	mol. ratio
	8	73,79	17,50			1,12	2,93		0,19	2,10	11,48		1
Iwaaka / Red	10	74,37	16,26	0,18		1,12	3,13		0,19	2,08	12,27		1
	12	66,67	24,26	0,33		0,95	2,60		0,17	1,92	10,99		0,7
Iwaki / Yellow	8	72,52	17,18	0,85	1,59				3,91		0,23	3,92	1
	10	64,95	23,89	1,50	2,33				3,55		0,23	3,39	0,7
	12	55,07	31,74	3,75	3,29				3,01		0,31	2,75	0,5
Gunjo / Blue	8	68,66	9,33		6,58			6,33	7,38		0,69		2
	10	68,99	8,66		5,40			7,31	7,61		0,80		2
	12	64,24	11,85		8,40			6,12	7,24		0,89		1,5

by PIXE elemental analysis: cadmium for cadmium red, antimony (and a small proportion of lead, probably) for yellow, cobalt and aluminum for cobalt blue.

3.3. EBS

As the main objective of this study was related to grain size investigation, only paints with close composition whatever the particle size were considered. For this reason, the yellow paints showing three different compositions for the three particle sizes were not selected for this section.

The EBS spectra for the paint layers prepared with the <code>Iwaaka/red</code> or the <code>Gunjo/</code>blue pigments are presented in Fig. 2. For all spectra, the edges of C, O and Pb were clearly identified; C and O originate from the linseed oil and Pb and O from the pigment. The edges of Si and minor elements were weaker and not clearly isolated. The shapes of the EBS spectra show different patterns even for paints of very close composition; these variations can be therefore attributed to the different grain sizes. The most significant difference was observed between the spectra corresponding to grain sizes of 13 μm and 26 μm .

This general trend observed experimentally for lead silicate paint is qualitatively similar to the simulations carried out by Mayer and Silva [19] for lead carbonate particles in linseed oil.

3.4. Simulation

The EBS simulated spectra for 3 MeV incident protons are shown in Fig. 3 for the paint layers prepared with the *Iwaaka*/red pigment.

For each simulation, the particle size was used as provided by the SEM observations. The density of each paint layer was calculated according to the pigment composition determined by PIXE. For the linseed oil matrix, the oxygen content was fitted at about two times higher than in linseed oil which is qualitatively consistent with the oxygen uptake during the drying process [32]. The pigment volume fraction (assumed to be 37 %) and the stick-out fraction (unknown) were adjusted to fit the experimental spectra. The obtained values were 18 vol% and 50–60 % of diameter, 20 vol% and 20 % of diameter, 30 vol% and 15 % of diameter for numbers 12, 10 and 8, respectively. The fitted volume fractions were lower than the expected values known from the preparation process of the paint; this difference has not yet been explained. The stick-out parameter and the elemental concentrations based on the PIXE results will be checked with further investigation.

Nevertheless, a reasonable agreement between experimental and simulated spectra was achieved with only a few free fit parameters (pigment volume fraction, stick-out fraction, oxygen content of oil). All other parameters were taken from SEM observations, PIXE results or from the literature. Differences between experimental and simulated spectra can be caused by the simplified model using spherical pigment

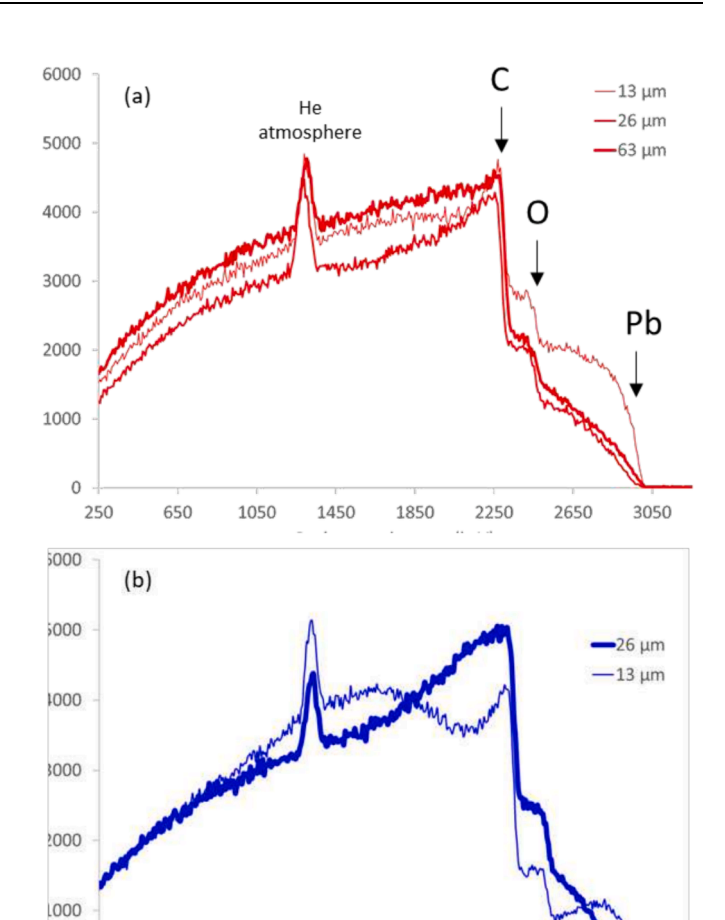


Fig. 2. Experimental spectra for 3 MeV H+ backscattered from thick layer of paints made of lead silicate-based pigments in linseed oil. The scattering angle was 130° and the experiments were carried out under helium atmosphere. (a) <code>Iwaaka/red</code> pigment numbers 8, 10 and 12; (b) <code>Gunjo/blue</code>, numbers 10 and 12.

1850

2250

2650

1450

Backscattered energy (keV)

particles: the resulting structures are shown in Fig. 4, but in reality, the shapes of the pigments deviate considerably from spheres for these lead silicate pigments (see Fig. 1).

250

650

1050

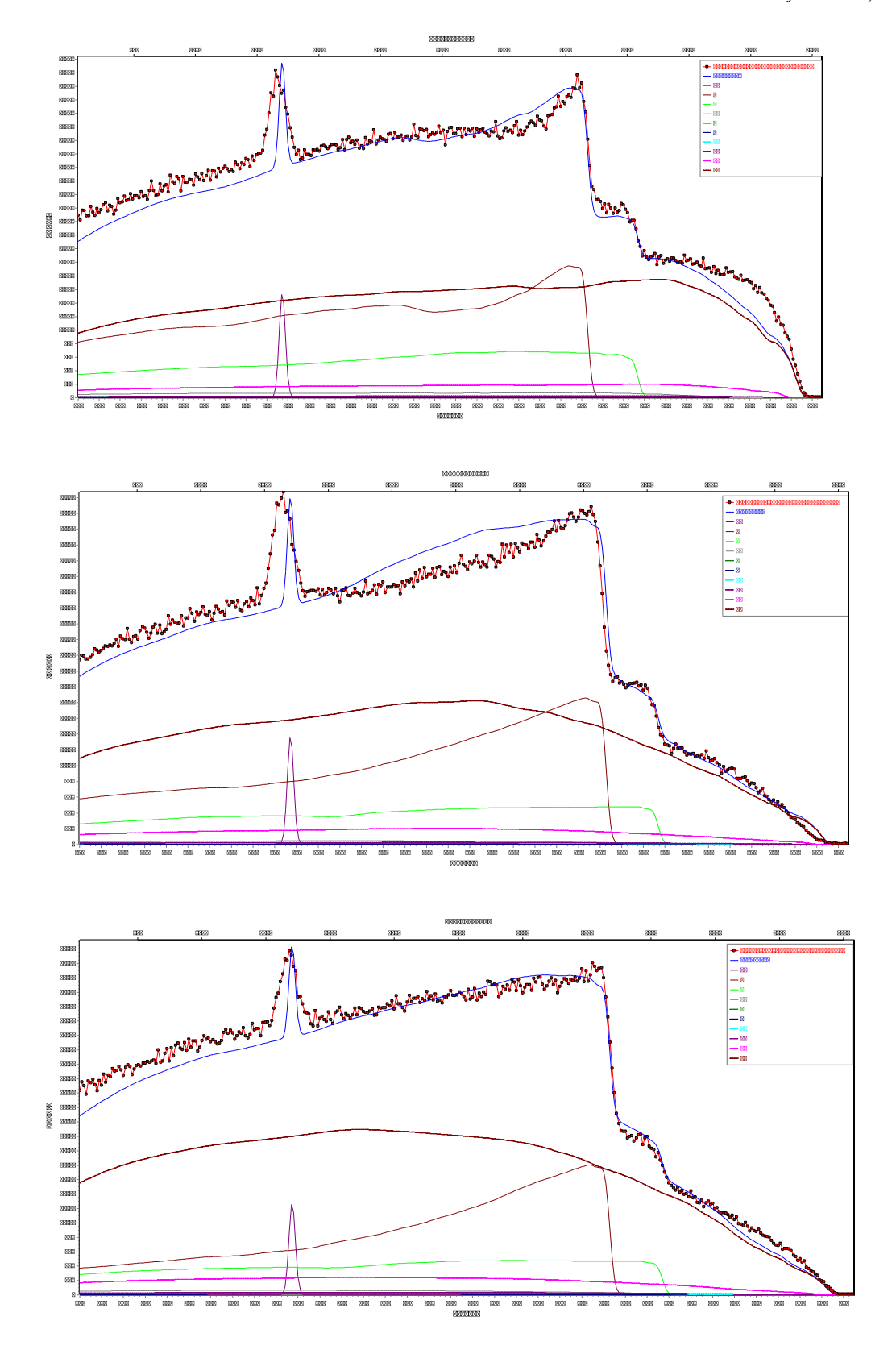


Fig. 3. Simulated EBS spectra for 3 MeV incident protons at a scattering angle of 130° for the paint layers prepared with the <code>Iwaaka/red</code> pigment. From top to bottom: pigment particle diameters are 13 ± 3 µm (number 12), 26 ± 4 µm (number 10) and 64 ± 23 µm (number 8).



Fig. 4. Visualization of the assumed paint layer structure (cross-section) used to simulate the EBS spectrum of the Iwaaka/red paint. From top to bottom, pigment particle distribution in the paint with three different pigment grain sizes: $13 \pm 3 \mu m$ (number 12), $26 \pm 4 \mu m$ (number 10) and $64 \pm 23 \mu m$ (number 8). The width of each cross-section is 4096 μm . White: pigment; Grey: oil; Sky blue: helium. Comparison with ongoing SEM observations on real sample cross-sections will help improve simulation.

4. Conclusions

Replications of paint layers using well-characterized pigments in linseed oil were produced. The composition of the pigment particles was characterized by PIXE, while the size distribution of the particles was evaluated by SEM.

Simulations of the EBS spectra were performed using the STRUCTNRA code using the knowledge from PIXE and SEM as input, thus strongly reducing the number of free parameters. A reasonable agreement between experimental and simulated spectra was achieved. This demonstrates that the simulation and quantitative understanding of EBS spectra from paintings requires taking the microstructure of the paint layer into account.

In an optimistic perspective, the good agreement between the simulation and the experimental data reveals the viability of specialized tools to analyze inhomogeneous samples. One of the limitation is the convergence time that is still prohibitive in practical applications, and would require human driven optimization. Nonetheless, the simulation tool opens a promising path for data processing based on machine learning algorithms, either by Bayesian optimization (given the high computational cost of each simulation) or by adopting deep neural networks (given the complexity and the nuances of experimental spectra for paint layers).

Differences between experimental and simulated spectra are probably caused by the simplified model using spherical pigment particles: in reality, the shapes of the pigment particles deviate considerably from spheres. Further investigations using experimental SEM sample cross-sections are ongoing. The main practical problem is the need for very large sample cross-sections (of at least a few mm) with sufficient resolution. This is a challenge for sample preparation and SEM investigations.

The current investigations and simulations will be extended to the blue pigment, and it is foreseen to investigate lead white samples with controlled grain size.

The results show that only the combination of the two IBA techniques together with SEM provides complete information on both the pigment and the binder.

Declaration of competing interest

The authors declare that they have no known competing financial interests or personal relationships that could have appeared to influence the work reported in this paper.

Acknowledgement

The authors thank the AGLAE group for assistance during the PIXE-EBS experiments, Eddy Foy (LAPA, NIMBE-IRAMAT) for the DRX measurement and Martin Balden (Max-Planck-Institut) for preliminary optical and SEM observations. This article is dedicated to the memory of Claire Berthier.

References

- C. Neelmeijer, I. Brissaud, T. Calligaro, A. Guy Demortier, M. Hautojärvi, L. Mäder, M. Martinot, T. Schreiner, G.W. Tuurnala, Paintings - A challenge for XRF and PIXE analysis, X-Ray Spectrom. 29 (2000) 101.
- [2] C. Andalò, M. Bicchieri, P. Bocchini, G. Casu, G.C. Galletti, P.A. Mandò, M. Nardone, A. Sodo, M. Plossi Zappalà, The beautiful "Trionfo d'Amore" attributed to Botticelli: a chemical characterisation by proton-induced X-ray emission and micro-Raman spectroscopy, Anal. Chim. Acta 429 (2001) 279.
- [3] A. Denker, J. Opitz-Coutureau, Paintings high-energy protons detect pigments and paint-layers, Nucl. Instr. Meth. B 213 (2004) 677.
- [4] P.A. Mandò, M.E. Fedi, N. Grassi, A. Migliori, Differential PIXE for investigating the layer structure of paintings, Nucl. Instr. Meth. B 239 (2005) 71.
- [5] P.A. Mandò, Nuclear physics and archaeometry, Nucl. Phys. A 751 (2005) 393c.
- [6] Ž. Šmit, et al., Concentration profiles in paint layers studied by differential PIXE, Nucl. Instr. Meth. B 266 (2008) 2047–2059.
- [7] T. Calligaro, et al., Emerging nuclear methods for historical painting authentication: AMS-14C dating, MeV-SIMS and O-PTIR imaging, global IBA, differential-PIXE and full-field PIXE mapping, Forensic Sci. Int. 336 (2022) 111327, https://doi.org/10.1016/j.forsciint.2022.111327.
- [8] J. Absil, H.-P. Garnir, D. Strivay, C. Oger, G. Weber, Study of color centers induced by PIXE irradiation, Nucl. Instrum. Meth. B 198 (2002) 90.
- [9] O. Enguita, T. Calderón, M.T. Fernández-Jiménez, P. Beneitez, A. Millan, G. García, Damage induced by proton irradiation in carbonate based natural painting pigments, Nucl. Instr. and Meth. B 219–220 (2004) 53.
- [10] L. Beck, P.C. Gutiérrez, F. Miserque, L. Thomé, Proton beam modification of lead white pigments, Nucl. Instr. Meth. B 307 (2013) 20.
- [11] T. Calligaro, et al., PIXE analysis of historical paintings: is the gain worth the risk? Nucl, Instr. and Meth. B 363 (2015) 135.
- [12] L. Beck, P.C. Gutiérrez, S. Miro, F. Miserque, Ion beam modification of zinc white pigment characterized by ex situ and in situ μ -Raman and XPS, Nucl. Instr. Meth. B 409 (2017) 96.
- [13] L. Beck, et al., IBA techniques: Examples of useful combinations for the characterisation of cultural heritage materials, Nucl Instruments and Methods in Physics Research B 269 (2011) 2999.
- [14] L. Beck, Recent trends in IBA for cultural heritage studies, Nucl. Inst. Methods Phys. Res. B 332 (2014) 439.
- [15] L. Beck, et al., New approaches for investigating paintings by ion beam techniques, Nucl. Instr. and Meth. in Physics Research. B 268 (2010) 2086.
- [16] L. de Viguerie, et al., Composition of renaissance paint layers: Simultaneous particle induced X-ray emission and backscattering spectrometry, Anal. Chem. 81 (2009) 7960.
- [17] L. Beck, C. Jeynes, N.P. Barradas, Characterization of paint layers by simultaneous self-consistent fitting of RBS/PIXE spectra using simulated annealing, Nucl. Instr. Meth. B 266 (2008) 1871.
- [18] S.L. Molodtsov, A.F. Gurbich, C. Jeynes, Accurate ion beam analysis in the presence of surface roughness, J. Phys. D: Appl. Phys. 41 (2008) 205303.
- [19] M. Mayer, T.F. Silva, Computer simulation of backscattering spectra from paint, Nucl. Instr. Meth. Phys. Res. B 406 (2017) 75.
- [20] M. Mayer, Computer simulation of ion beam analysis of laterally inhomogeneous materials, Nucl. Instr. Meth. B 371 (2016) 90.
- [21] http://nakagawa-gofun.co.jp/english/begin/manufacture.html.
- [22] L. Chua, et al., Investigating the colour difference of old and new blue Japanese glass pigments for artistic use, J. Conserv. Sci. 38 (2022) 1.
- [23] L. Pichon, B. Moignard, Q. Lemasson, C. Pacheco, P. Walter, Development of a multi-detector and a systematic imaging systemon the AGLAE external beam, Nucl. Inst. Methods Phys. Res. B 318 (2014) 27.
- [24] L. Pichon, T. Calligaro, Q. Lemasson, B. Moignard, C. Pacheco, Programs for visualization, handling and quantification of PIXE maps at the AGLAE facility, Nucl. Inst. Methods Phys. Res. B 363 (2015) 48.
- [25] J.L. Campbell, D.J.T. Cureatz, E.L. Flannigan, C.M. Heirwegh, J.A. Maxwell, J. L. Russell, S.M. Taylor, The Guelph PIXE software package V, Nucl. Inst. Methods Phys. Res. B 499 (2021) 77, https://doi.org/10.1016/j.nimb.2021.05.004.
- [26] M. Mayer, Improved physics in SIMNRA 7, Nucl. Instr. Meth. B 332 (2014) 176.
- [27] M. Mayer, P. Malinsky, F. Schiettekatte, Z. Zolnai, Intercomparison of ion beam analysis software for the simulation of backscattering spectra from twodimensional structures, Nucl. Instr. Meth. B 385 (2016) 65.
- [28] O.L.G. Alderman, et al., J. Am. Ceram. Soc. 105 (2022) 938.
- [29] J.F. Ziegler, SRIM-2003, Nucl. Instr. Meth. B 219–220 (2004) 1027.

- [30] A.F. Gurbich, SigmaCalc recent development and present status of the evaluated cross-sections for IBA, Nucl. Instr. Meth. B 371 (2016) 27.
- [31] E.L. Flannigan, J.L. Campbell, Emulation of the Curiosity rover alpha particle X-ray spectrometer with accelerator-based PIXE: Implications for calibration, Nucl. Instr. Meth. B 413 (2017) 19–26.
- [32] S. Pizzimenti, L. Bernazzani, M. Rosaria Tinè, V. Treil, C. Duce, I. Bonaduce, Oxidation and cross-linking in the curing of air-drying artists' oil paints, ACS Appl. Polym. Mater. 3 (4) (2021) 1912.